

Super-Jeans fragmentation in massive star-forming regions revealed by triangulation analysis

GUANG-XING LI ^{1,*} MENGKE ZHAO ^{2,1} AND XING LU ³

¹South-Western Institute For Astronomy Research, Yunnan University, Kunming 650600, China

²School of Astronomy and Space Science, Nanjing University, 163 Xianlin Avenue, Nanjing 210023, People's Republic of China

³Shanghai Astronomical Observatory, Chinese Academy of Sciences, Shanghai, People's Republic of China

ABSTRACT

Understanding the fragmentation of the gas cloud and the formation of massive stars remains one of the most challenging questions of modern astrophysical research. Either the gas fragmentation in a Jeans-like fashion, after which the fragments grow through accretion, or the fragmentation length is larger than the Jeans length from the start. Despite significant observational efforts, a consensus has not been reached. The key is to infer the initial density distribution upon which gravitational fragmentation occurs. Since cores are the products of the fragmentation process, the distances between adjacent cores serve as a scale indicator. Based on this observation, we propose a Delaunay triangulation-based approach to infer the density structure before the fragmentation and establish the link between density distribution and gas fragmentation length. We find that at low density, the fragmenting is Jeans-like, and at high densities, the core separations are larger than the prediction of the Jeans fragmentation. This super-Jeans fragmentation, which often occurs in groups, is responsible for the clustered formation of massive stars.

1. INTRODUCTION

Star forms from the collapse of gas clouds, which are complex, multi-scale systems. Understanding how such a system evolves remains one of the most difficult challenges in astrophysical research. Massive stars have masses larger than the Jeans mass of clouds. The Jeans mass [Jeans \(1902\)](#) is the characteristic mass of gravitational instability, and to explain the formation of massive stars, one needs to explain how massive stars can acquire masses much larger than the Jeans mass. There are two possibilities: The first [Bonnell et al. \(2001\)](#) assumes that massive stars start with cores whose masses are comparable to the Jeans mass. Since the Jean mass is small, these cores must accrete significant mass before becoming stars. Another possibility is to form cores whose masses are much larger than the Jeans mass from the start [Vázquez-Semadeni et al. \(2019\)](#); [Padoan et al. \(2020\)](#). In the latter case, the fragmentation occurs at a scale much larger than the Jeans length – a phenomenon that we call super-Jeans fragmentation. The key to understanding massive star formation is distinguishing between Jeans and super-Jeans fragmentation. Despite years of research, both Jean-like fragmentation ([Liu et al. 2017](#); [Sanhueza et al. 2019](#); [Svoboda et al. 2019](#); [Lu et al. 2020](#)) and super-Jeans fragmentation ([Zhang et al. 2009](#); [Wang et al. 2014](#); [Figueira et al. 2018](#); [Xu et al. 2023](#)) has been reported, and no conclusion has been reached.

One key step to make such a distinction is to infer the gas densities before fragmentation occurs. However, due to the highly complex density distribution of the star-forming regions, estimating this initial density distribution is difficult. In previous works, it is assumed that fragmentation takes place at a region of a constant density [Lu et al. \(2020\)](#), where the fragmentation length does appear to be similar to the Jeans length. The density is estimated at a scale comparable to the core separation, super-Jeans fragmentation is observed [Xu et al. \(2023\)](#). The key to distinguishing between different fragmentation mechanisms is to construct the initial density distribution.

In this paper, we combine Delaunay triangulation [Delaunay \(1934\)](#) and Voronoi diagram [Voronoi \(1908\)](#) to infer the initial density structure Delaunay triangulation is an algorithm to construct a triangulation meshes from sets of points and Voronoi diagrams are methods to divide a region based on sets of points. We use the Delaunay triangulation to infer the fragmentation length [Li et al. \(2021\)](#), and combine it with the Voronoi diagram to infer the gas density.

* E-mail: gqli@ynu.edu.cn, ligx.ngc7293@gmail.com(G-XL); South-Western Institute For Astronomy Research, Yunnan University, Kunming 650600, China

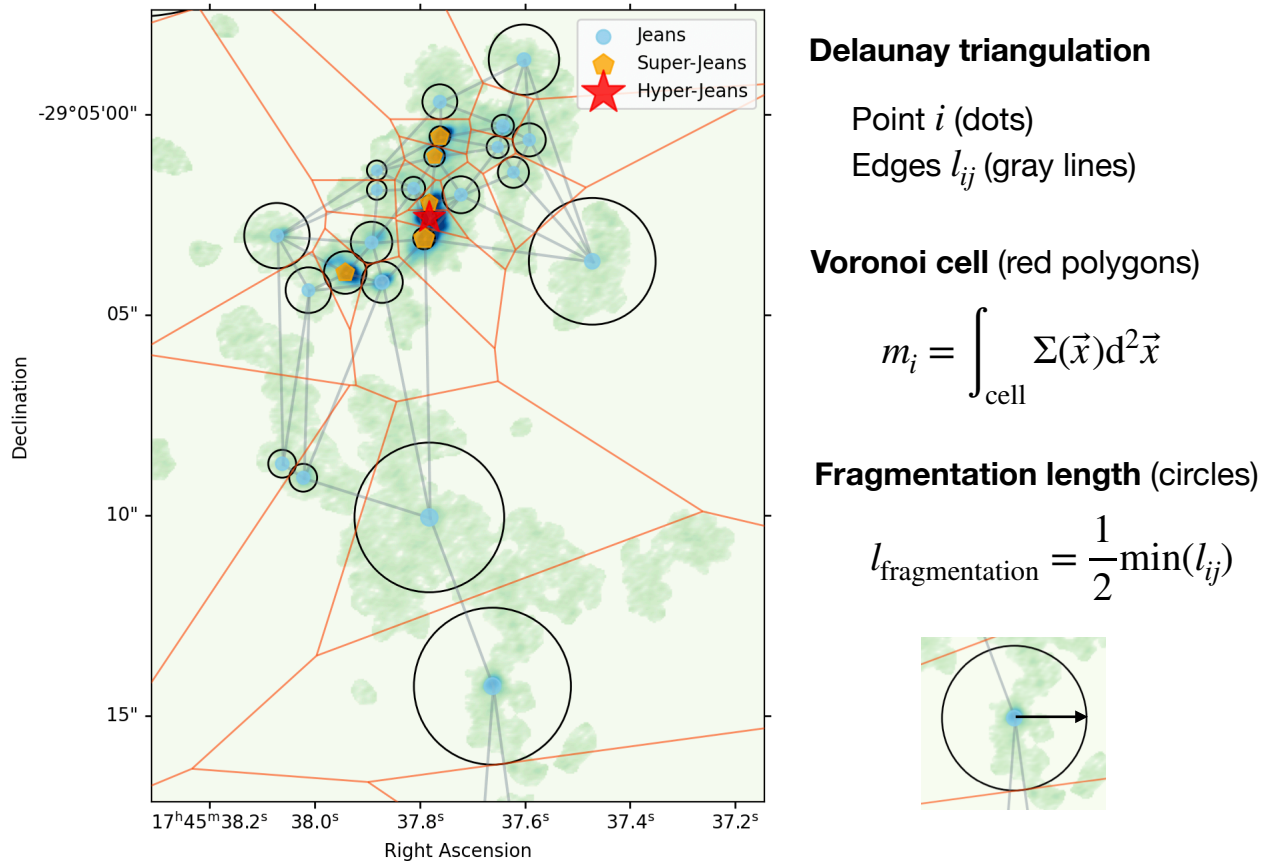


Figure 1. Measuring the fragmentation length and mass. Starting with a catalog containing the positions of the cores, we construct the Delaunay triangulation (gray lines) and Voronoi diagram (red lines). We use the Voronoi diagram to compute the masses of the regions $m_{i,\text{map}}$, and use the Delaunay triangulation to estimate the sizes of the regions l_i , which are indicated using circles.

This approach allows us to compare the spatial distribution of cores with the predictions of Jeans criterion with unprecedented accuracy.

2. METHOD & RESULTS

We use ALMA observations toward three massive star-forming regions in the center of the Galaxy [Lu et al. \(2020\)](#). The data have a resolution of $0.0025'' \times 0.0017''$ (equivalent to $2000 \text{ AU} \times 1400 \text{ AU}$ at a distance of 8.178 kpc [GRAVITY Collaboration et al. \(2019\)](#)), and an image rms measured in emission-free regions without primary-beam corrections of $40 \mu\text{Jy dbeam}^{-1}$. We use the catalog and the dust continuum map to trace the gas and study fragmentation.

Table 1. Summary of different fragmentation modes. f_{Jeans} is defined in Eq. 6.

Mode	Definition	M_{core}
Jeans fragmentation	$f_{\text{Jeans}} < 2$	$1M_{\odot}$
Super-Jeans fragmentation	$2 < f_{\text{Jeans}} < 4$	$10M_{\odot}$
Hyper-Jeans fragmentation	$f_{\text{Jeans}} < 4$	$30M_{\odot}$

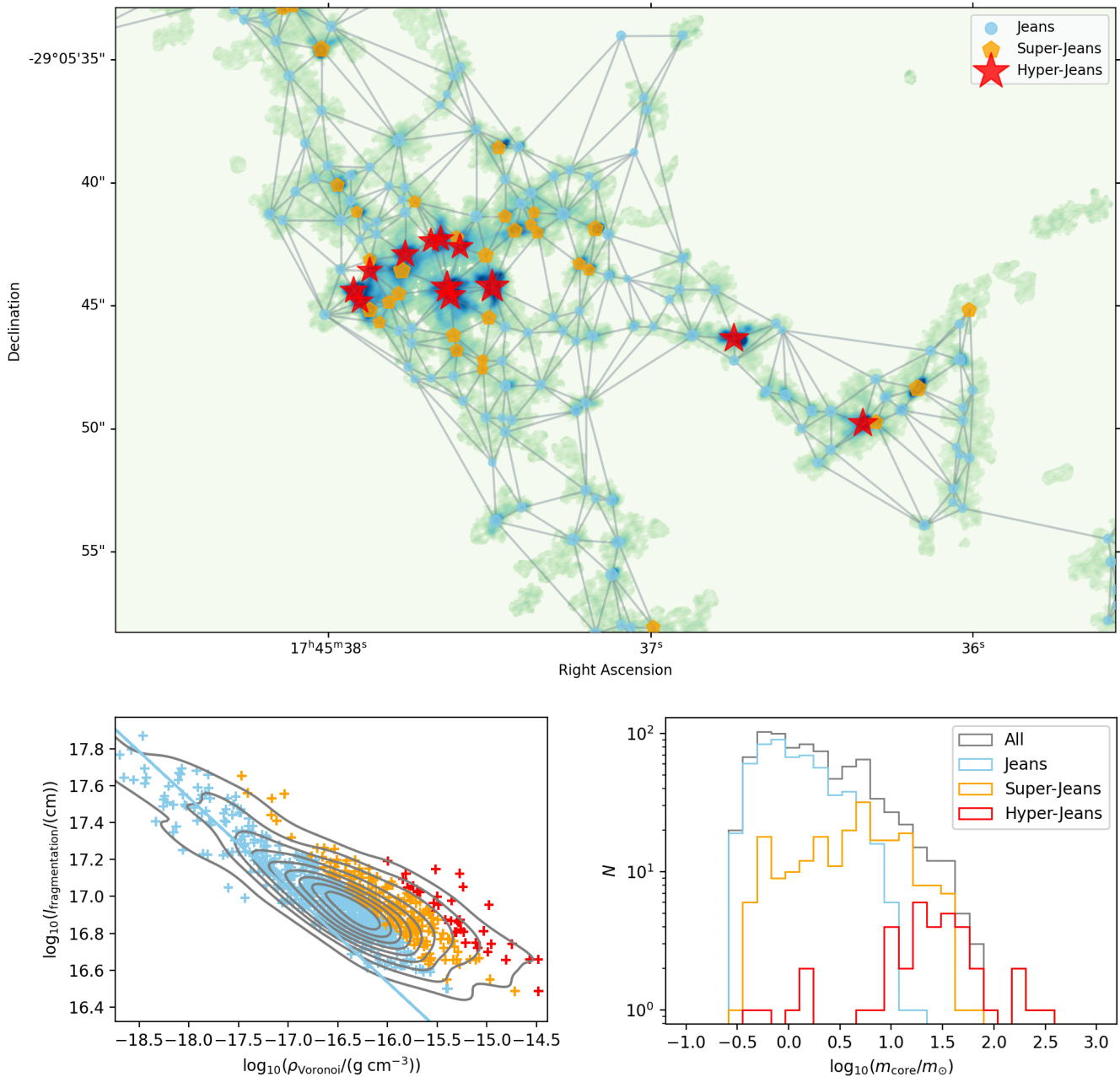


Figure 2. Jeans, super-Jeans and hyper-Jeans fragmentation. In the upper panel, we plot the surface density map and spatial distribution of cores in a CMZ cloud called the 20 km s^{-1} cloud. The background image is a map of the surface density distribution. Different symbols represent different cores. The lines represent the Delaunay triangulation, through which the fragmentation length is inferred. Different symbols represent cores produced by Jeans, super-Jeans, and hyper-Jeans fragmentation.

2.1. Estimating Density field and fragmentation length

To compute the fragmentation scale, we use Delaunay triangulation [Delaunay \(1934\)](#), which is a technique for creating a mesh of contiguous, non-overlapping triangles from a dataset of points. Towards each data point, the triangulation mesh provides the locations of its closest neighbors. Toward a point (vertex) p_i , the triangulation provides the indexes

and locations of its neighbors. Assuming that the distances to the neighbors are d_{ij} , the radius of a region is

$$r_{i,\text{Delaunay}} = \min_j(d_{ij}) , \quad (1)$$

where i is the point of the interest, and j represent its neighbors. The fragmentation length is

$$l_{\text{fragmentation}} = 2 r_{\text{Delaunay}} . \quad (2)$$

To compute the mass, use the Voronoi diagram [Voronoi \(1908\)](#), which is a method to divide a plane into regions based on a given set of objects. For each vertex point p_i , the Voronoi diagram provides a region S_i which is associated with the region, and the mass of the vertex point is

$$m_{i,\text{Voronoi}} = \int_{S_i} \Sigma(x,y) dx dy \quad (3)$$

where Σ is the surface density distribution. The calculations are performed with `SCIPY.SPATIAL` package. The definitions of these quantify are illustrated in Fig. 1. We note that computation of the $m_{i,\text{Voronoi}}$ is necessary because all the masses contribute to gravity. A comparison between the mass of the core m_{core} derived using `DENDROGRAM` ([Rosolowsky et al. 2008](#)) which is core extraction algorithm and the mass of the Voronoi regions m_{Voronoi} is presented in Fig. 5, the difference between m_{core} and m_{Voronoi} is significant, particularly towards low-mass cores. Details on mass calculation, including the conversion from flux to surface density and a step where we remove noisy parts of the map from our analysis are presented in Appendix A.

The initial density can be estimated as

$$\rho_{i,\text{Voronoi}} = \frac{m_{i,\text{Voronoi}}}{4/3\pi r_i^3} . \quad (4)$$

If the fragmentation is Jeans-like, we expect

$$l_{i,\text{fragmentation}} = \frac{\pi^{1/2} c_s}{\sqrt{G\rho_i}} , \quad (5)$$

where $c_s = \sqrt{k_B T_{\text{gas}}/m_{\text{H}_2}}$ is the thermal sound speed, k_B is the Boltzmann constant, T_{gas} is the temperature of the gas, and m_{H_2} is the mass of the H_2 gas. We assume $T_{\text{gas}} = 100$ K, which is a value agreed upon by the literature [Henshaw et al. \(2023\)](#).

In Fig. 2 we plot the relation between density and fragmentation length. We find that in general, the fragmentation roughly follows the prediction of the Jeans fragmentation, where a larger density is related to a smaller fragmentation length. In addition, we observe that a significant fraction of cores with total masses $m_{i,\text{Voronoi}}$ larger than the Jeans mass. To quantify this excess at high densities, we use the term ‘‘super-Jeans fragmentation’’ to refer to cores with $d_{\text{fragmentation}} = 2 r_{\text{Delaunay}} > 2 l_{\text{Jeans}}$, and ‘‘hyper-Jeans fragmentation’’ to refer to cores with $l_{\text{core}} > 4 l_{\text{Jeans}}$. Since $m \sim \rho l^3$, cores produced from these fragmentation modes have masses orders of magnitudes larger than the Jeans mass. These different modes are summarized in Table 1. From a breakdown of cores under different fragmentation modes (Fig. 2), where low-mass cores are produced by Jeans fragmentation and cores of higher masses are produced by super and hyper-Jeans fragmentation.

From a breakdown of core masses in these different categories (Fig. 2), we find that in the case of CMZ clouds, Jeans-fragmentation dominates the production of $2 m_{\odot}$ cores, super-Jeans fragmentation dominates the production of $10 m_{\odot}$ cores, and hyper-Jeans fragmentation dominates the production $30 m_{\odot}$ cores. The formation of high-mass cores is dominated by super-Jeans fragmentation.

To quantify the fragmentation, we introduce a parameter called the Jeans ratio, which is the ratio between the observed fragmentation length and the Jeans length, and by plotting f_{Jeans} against ρ (Fig. 3) we find that the trend is can be well-describes by

$$f_{\text{Jeans}} = \max \left(\frac{l_{\text{fragmentation}}}{l_{\text{Jeans}}} = \left(\frac{\rho}{10^{-17} \text{g cm}^{-3}} \right)^{1/3}, 0 \right) , \quad (6)$$

where the fragmentation mass is

$$m_{\text{super}} = \frac{c_s^3}{G^{3/2} \rho^{1/2}} f_{\text{Jeans}}^3 = m_{\text{Jeans}} f_{\text{Jeans}}^3 \propto \rho^{1/2} . \quad (7)$$

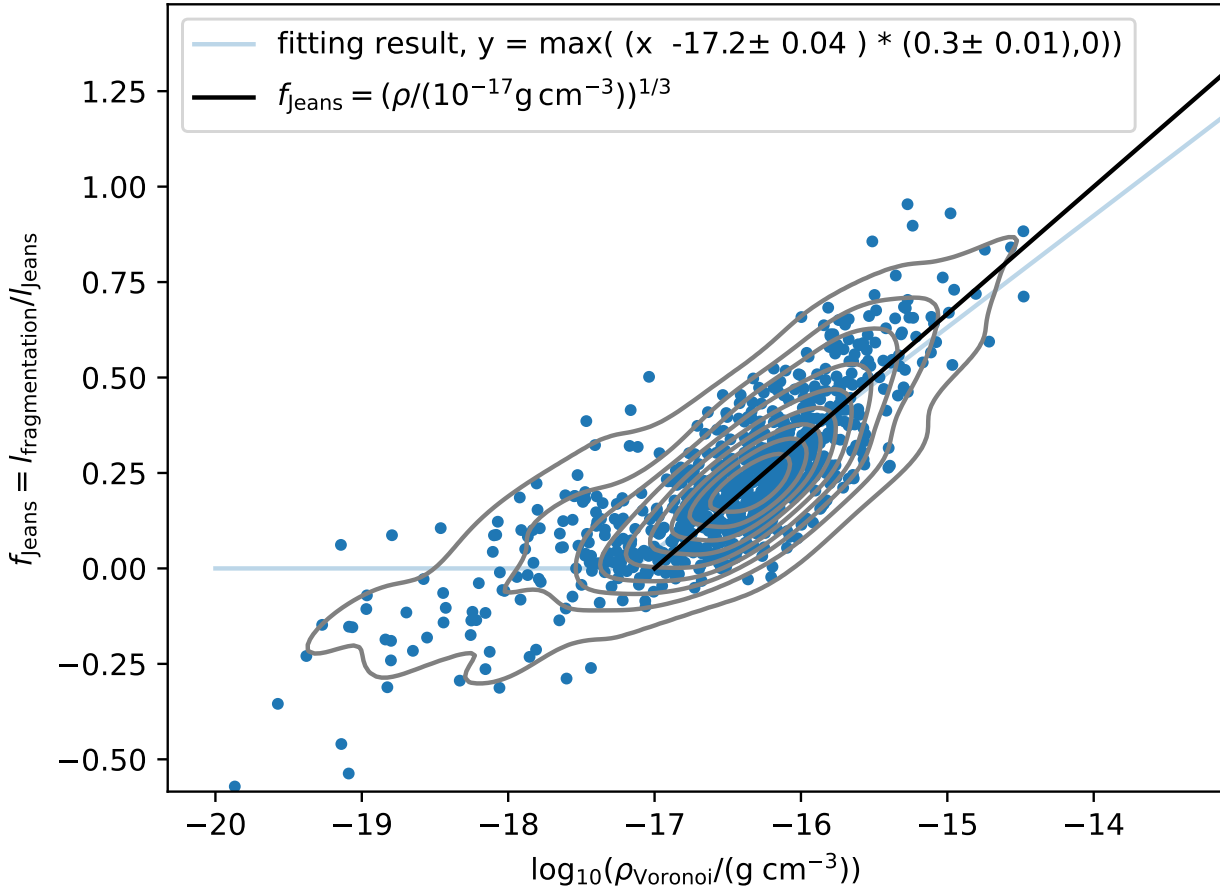


Figure 3. Jeans fraction $f_{\text{Jeans}} = l_{\text{fragmentation}}/l_{\text{Jeans}}$ as a function of gas density. The line describes the proposed correlation where $f_{\text{Jeans}} \propto \rho^{1/3}$.

Since $f_{\text{Jeans}} \propto \rho^{1/3}$, we expect $m \propto \rho^{1/2}$, high-mass cores form at high-density environment.

We also find that the super-Jeans fragmentation has a clustered distribution. In Fig. 2, we use different colors and symbols to represent cores produced from different fragmentation modes. The super-Jeans fragmentation tends to occur in groups, with hyper-Jeans cores located at the center and super-Jeans cores located at the outside. This spatial arrangement suggests a link between the flow structure at the larger scale and super-Jeans fragmentation at the center. This spatial arrangement also suggests that the phenomena of mass segregation [Bonnell & Davies \(1998\)](#) of star clusters, where massive stars stay at central locations as compared to low-mass stars, is primordial [Motherway et al. \(2023\)](#); [Xu et al. \(2024\)](#).

There are a few physical mechanisms that can explain the formation of super-Jeans fragmentation. For example, it is proposed that the fragmentation is detailed, leading to a more massive object [Vázquez-Semadeni et al. \(2019, 2023\)](#), and [Padoan et al. \(2020\)](#) proposed an inertia flow mode. Our findings can be tested against simulation results in the future. In a recent paper, [Li 2024](#) derived non-stationary corrections, the Jeans ratio becomes

$$f_{\text{Jeans}} = (t_{\text{ff}}/t_{\text{acc}})^{1/3}, \quad (8)$$

where $t_{\text{acc}} = \rho/\dot{\rho}$. A positive $\dot{\rho}$ leads to a larger fragmentation length.

Letting

$$f_{\text{Jeans}} \propto \rho^{1/3}, \quad (9)$$

we expect

$$t_{\text{acc}} \propto \rho^{-1.5}, \dot{\rho} \propto \rho^{2.5} \quad (10)$$

where the high-density region should have a high rate of density increase to ensure super-Jeans fragmentation. The super-Jeans fragmentation can be related to the dynamic nature of the high-density regions. This can be explained if the whole region is collapsing globally. Super and hyper-Jeans fragmentation occurs at the central regions where the flow converges, and Jeans fragmentation occurs at the outside. Other processes such as core accretion and further evolution of core separations, can also move the cores around in the $\rho_{\text{Voronoi}}-l_{\text{fragmentation}}$ diagram (Fig. 2), and can potentially explain the super-Jeans accretion.

3. CONCLUSION

The fragmentation of gas clouds and the formation of massive stars is one of the most complex astrophysical processes. The Jeans criterion sets the foundation of gravitational fragmentation, yet the observational results remain inclusive. Fragmentation is the process that links an initial density distribution, which is produced by e.g. turbulence and global collapse, to a set of regions that collapse on their own. Previous studies assumed flat initial density distributions, neglecting the internal density distributions. By developing a new adaptive approach based on the Delaunay triangulation and Voronoi diagram, we estimate the initial density structure, and study gravitational fragmentation with a much-improved accuracy.

We find that at the low-density end, the fragmentation is Jeans-like; at the high-density end, we observe a significant fraction of massive cores produced by fragmentation whose scales are much larger than the Jeans fragmentation. We use $f_{\text{Jeans}} = l_{\text{fragmentation}}/l_{\text{Jeans}}$ to describes deviations from the Jeans fragmentation, and find that $f_{\text{Jeans}} \propto \rho^{1/3}$. We also study the spatial distribution of super-Jeans cores and find that they are clustered at the center of the star-forming regions, leading to the clustered formation of massive stars.

The paper demonstrates the power of numerical methods developed in computational geometry, such as Delaunay triangulation and Voronoi diagram in analyzing complex patterns that emerged in modern astrophysical research, where effective ways to quantifying these complex structures is a key step towards physical understanding.

ACKNOWLEDGEMENTS

GXL acknowledges support from NSFC grant No. 12273032 and 12033005. X.L. acknowledges support from the National Key R&D Program of China (No. 2022YFA1603101), the Strategic Priority Research Program of the Chinese Academy of Sciences (CAS) Grant No. XDB0800300, the National Natural Science Foundation of China (NSFC) through grant Nos. 12273090 and 12322305, the Natural Science Foundation of Shanghai (No. 23ZR1482100), and the CAS ‘‘Light of West China’’ Program No. xzbzg-zdsys-202212.

REFERENCES

- Bonnell, I. A., Bate, M. R., Clarke, C. J., & Pringle, J. E. 2001, *MNRAS*, 323, 785, doi: [10.1046/j.1365-8711.2001.04270.x](https://doi.org/10.1046/j.1365-8711.2001.04270.x)
- Bonnell, I. A., & Davies, M. B. 1998, *MNRAS*, 295, 691, doi: [10.1046/j.1365-8711.1998.01372.x](https://doi.org/10.1046/j.1365-8711.1998.01372.x)
- Delaunay, B. 1934, *Bulletin de l’Academie des Sciences de l’URSS. Classe des sciences mathematiques et na*, 1934, 793
- Figueira, M., Bronfman, L., Zavagno, A., et al. 2018, *A&A*, 616, L10, doi: [10.1051/0004-6361/201832930](https://doi.org/10.1051/0004-6361/201832930)
- GRAVITY Collaboration, Abuter, R., Amorim, A., et al. 2019, *A&A*, 625, L10, doi: [10.1051/0004-6361/201935656](https://doi.org/10.1051/0004-6361/201935656)
- Henshaw, J. D., Barnes, A. T., Battersby, C., et al. 2023, in *Astronomical Society of the Pacific Conference Series*, Vol. 534, *Protostars and Planets VII*, ed. S. Inutsuka, Y. Aikawa, T. Muto, K. Tomida, & M. Tamura, 83, doi: [10.48550/arXiv.2203.11223](https://doi.org/10.48550/arXiv.2203.11223)
- Jeans, J. H. 1902, *Philosophical Transactions of the Royal Society of London Series A*, 199, 1, doi: [10.1098/rsta.1902.0012](https://doi.org/10.1098/rsta.1902.0012)
- Li, G.-X. 2022, *ApJS*, 259, 59, doi: [10.3847/1538-4365/ac4bc4](https://doi.org/10.3847/1538-4365/ac4bc4)
- Li, G.-X., Cao, Y., & Qiu, K. 2021, *ApJ*, 916, 13, doi: [10.3847/1538-4357/ac01d4](https://doi.org/10.3847/1538-4357/ac01d4)
- Liu, T., Lacy, J., Li, P. S., et al. 2017, *ApJ*, 849, 25, doi: [10.3847/1538-4357/aa8d73](https://doi.org/10.3847/1538-4357/aa8d73)
- Lu, X., Cheng, Y., Ginsburg, A., et al. 2020, *ApJL*, 894, L14, doi: [10.3847/2041-8213/ab8b65](https://doi.org/10.3847/2041-8213/ab8b65)

- Motherway, E., Geller, A. M., Childs, A. C., Zwicker, C., & von Hippel, T. 2023, arXiv e-prints, arXiv:2308.13520, doi: [10.48550/arXiv.2308.13520](https://doi.org/10.48550/arXiv.2308.13520)
- Ossenkopf, V., & Henning, T. 1994, *A&A*, 291, 943
- Padoan, P., Pan, L., Juvela, M., Haugbølle, T., & Nordlund, Å. 2020, *ApJ*, 900, 82, doi: [10.3847/1538-4357/abaa47](https://doi.org/10.3847/1538-4357/abaa47)
- Rosolowsky, E. W., Pineda, J. E., Kauffmann, J., & Goodman, A. A. 2008, *ApJ*, 679, 1338, doi: [10.1086/587685](https://doi.org/10.1086/587685)
- Sanhueza, P., Contreras, Y., Wu, B., et al. 2019, *ApJ*, 886, 102, doi: [10.3847/1538-4357/ab45e9](https://doi.org/10.3847/1538-4357/ab45e9)
- Svoboda, B. E., Shirley, Y. L., Traficante, A., et al. 2019, *ApJ*, 886, 36, doi: [10.3847/1538-4357/ab40ca](https://doi.org/10.3847/1538-4357/ab40ca)
- Vázquez-Semadeni, E., Gómez, G. C., & González-Samaniego, A. 2023, arXiv e-prints, arXiv:2306.13846, doi: [10.48550/arXiv.2306.13846](https://doi.org/10.48550/arXiv.2306.13846)
- Vázquez-Semadeni, E., Palau, A., Ballesteros-Paredes, J., Gómez, G. C., & Zamora-Avilés, M. 2019, *MNRAS*, 490, 3061, doi: [10.1093/mnras/stz2736](https://doi.org/10.1093/mnras/stz2736)
- Voronoi, G. 1908, *Journal für die reine und angewandte Mathematik (Crelles Journal)*, 1908, 97, doi: [doi:10.1515/crll.1908.133.97](https://doi.org/10.1515/crll.1908.133.97)
- Wang, K., Zhang, Q., Testi, L., et al. 2014, *MNRAS*, 439, 3275, doi: [10.1093/mnras/stu127](https://doi.org/10.1093/mnras/stu127)
- Xu, F., Wang, K., Liu, T., et al. 2024, *ApJS*, 270, 9, doi: [10.3847/1538-4365/acfee5](https://doi.org/10.3847/1538-4365/acfee5)
- Xu, F.-W., Wang, K., Liu, T., et al. 2023, *MNRAS*, 520, 3259, doi: [10.1093/mnras/stad012](https://doi.org/10.1093/mnras/stad012)
- Zhang, Q., Wang, Y., Pillai, T., & Rathborne, J. 2009, *ApJ*, 696, 268, doi: [10.1088/0004-637X/696/1/268](https://doi.org/10.1088/0004-637X/696/1/268)

APPENDIX

A. GAS MASS MEASUREMENT

We use the dust continuum map from an ALMA observation towards the center of our Galaxy [Lu et al. \(2020\)](#) to derive the total mass of the fragments. We compute the surface density map, we use the equation

$$\Sigma = R \frac{F_\nu}{B_\nu(T)\kappa_\nu}, \quad (\text{A1})$$

where F_ν is the flux density, $B_\nu(T)$ is the Planck function and κ is the dust emissivity, and R is the gas-to-dust mass ratio. We assume $R = 100$, $\kappa_\nu = 0.9 \text{ g cm}^{-1}$ [Ossenkopf & Henning \(1994\)](#).

Note that the map contains a significant amount of correlated noises in regions of low signal-to-noise ratios. To achieve improved accuracy, we remove these empty regions from our analysis by creating a mask where most of the emission is included. To achieve this, we use the method of CONstrained Diffusion Decomposition [Li \(2022\)](#) to decompose the input maps into component maps that contain structures at different scales, and the threshold is selected at the $n = 4$ component (which has a resolution of $2^4 = 16$ pixels) at a threshold of 1,2,1,2 mJy Beam $^{-1}$ for observations towards 20 km/s cloud, 50 km/s cloud, SgrC and SgrB1 respectively. This procedure is illustrated in [Fig 4](#).

B. MASS CORRECTIONS

In [Fig. 5](#) we present a comparison between the mass of the core m_{core} , as derived in [Lu et al. 2020](#) [Lu et al. \(2020\)](#), with the mass derived by summing over all the emission contained in the corresponding region in the Voronoi diagram v_{Voronoi} . The mass in the Voronoi diagram region is significant, particularly towards cores of smaller masses.

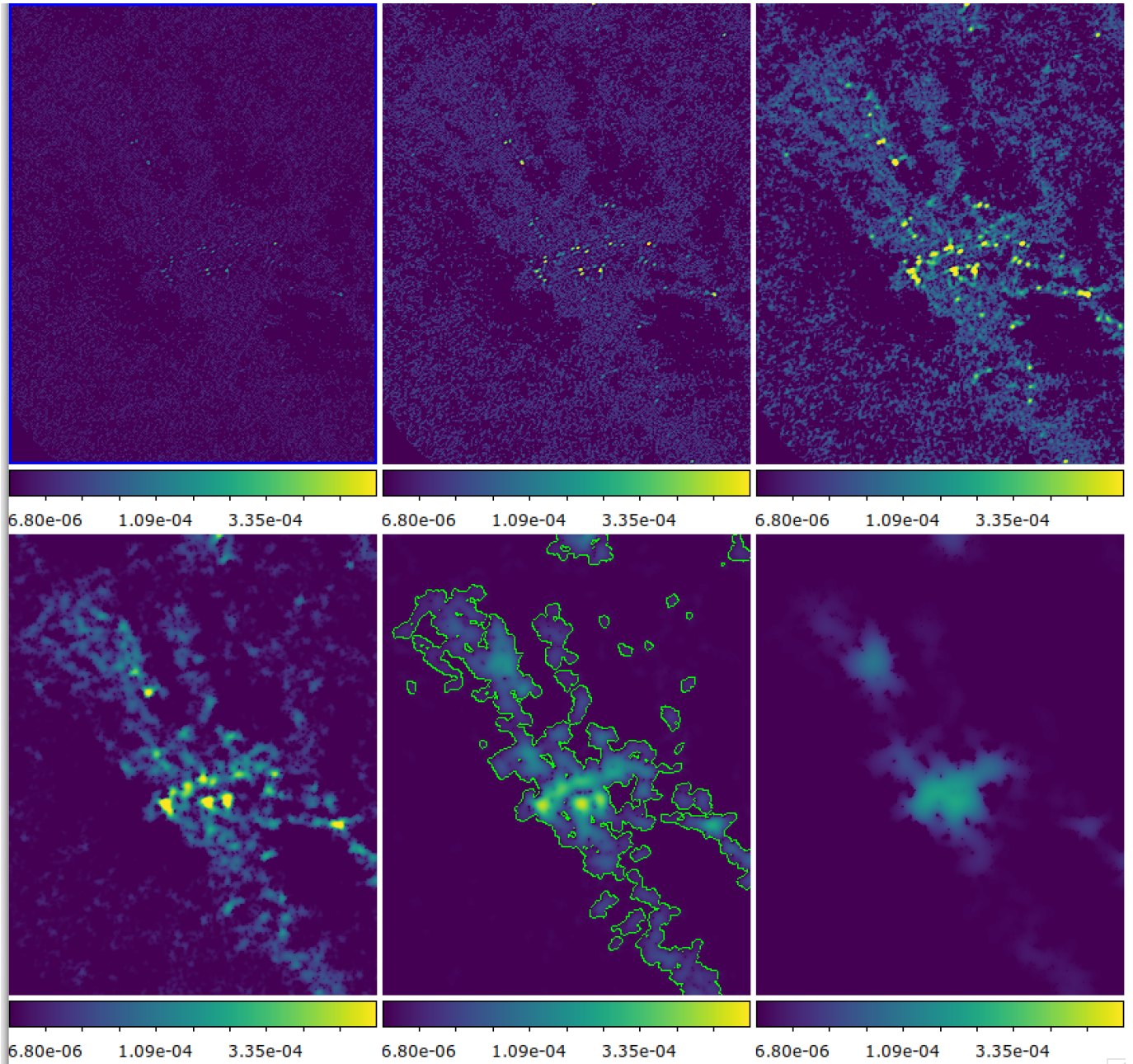


Figure 4. Method of creating a mask where most of the significant emission is include. We first decompose the map using the method of CONSTRAINED DIFFUSION DECOMPOSITION Li (2022). Then the a is created at the 4th component, at the threshold of 1 mJy Beam^{-1} . The boundaries of this mask is indicated using green contours in the 5th plot. The data shown here is taken at observations towards 20 km/s cloud from Lu et al. (2020).

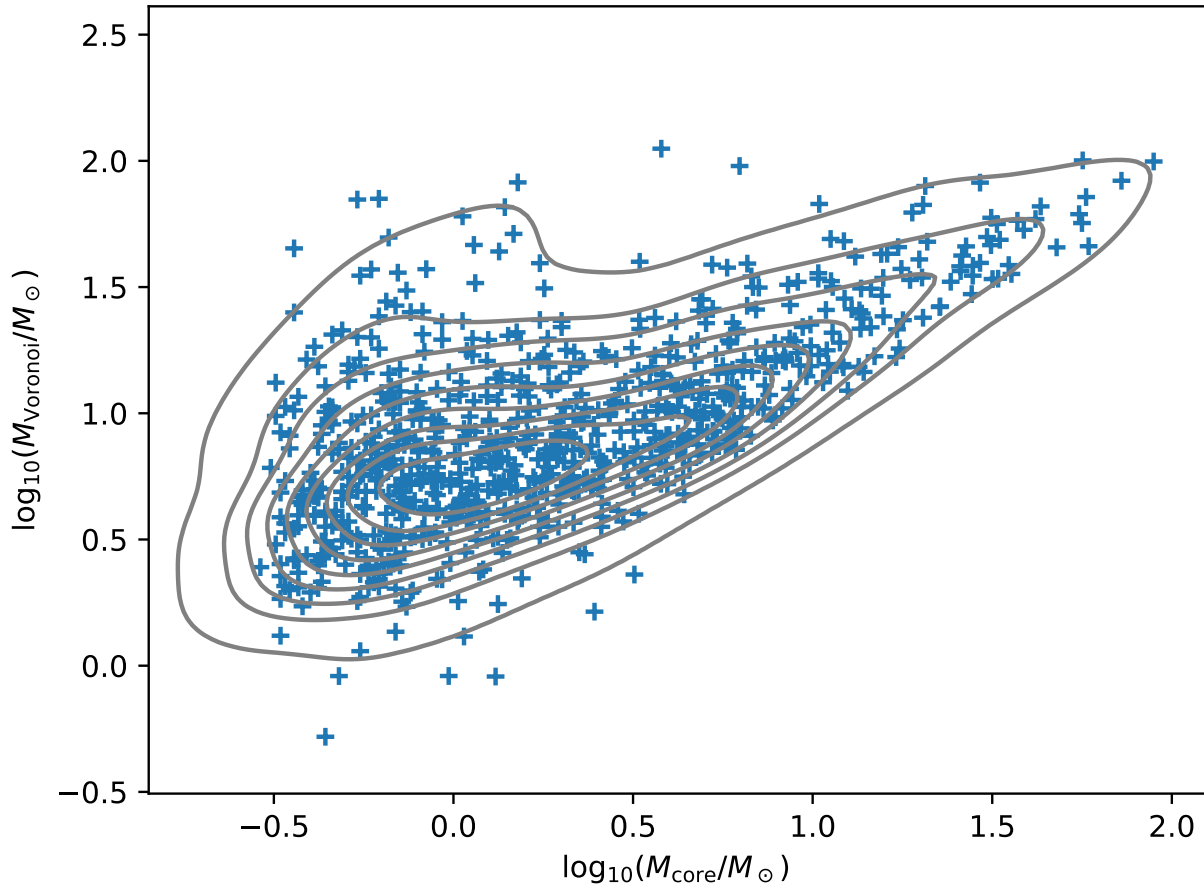


Figure 5. Fragmentation mass m_{map} plotted against the core mass m_{core} . Fragmentation mass m_{map} derived by summing over all the region partition produced using the Voronoi diagram, plotted against the masses of cores m_{core} . The differences between these two are caused by diffuse emissions outside the cores.